



**Cardiff University School of Physics and Astronomy  
MSc Research Project**

**Homodyne Kinetic Inductor Readout  
Analysis and Calibration**

**Deepika Velusamy  
Student Number: 1966924**

**Supervisor: Simon Doyle**

**28<sup>th</sup> June 2021**

# Contents

<b>1</b>	<b>Introduction</b>	<b>1</b>
1.1	Aim . . . . .	1
1.2	Objective . . . . .	2
<b>2</b>	<b>Précis of literature</b>	<b>3</b>
2.1	Kinetic Inductance . . . . .	3
2.2	Superconducting Microresonator . . . . .	4
2.3	Transmission lines . . . . .	4
2.4	Vector Network Analyzer . . . . .	5
2.5	Scattering Matrix . . . . .	5
2.6	Principle Of S-parameter . . . . .	5
2.7	Calculating Scattering Parameter In Microwave Circuit . . . . .	6
2.8	Introduction To Microwave Mixer . . . . .	7
2.9	Mixers . . . . .	7
2.9.1	Down Conversion Mixer . . . . .	7
2.10	IQ Mixers . . . . .	8
2.11	IQ circle . . . . .	9
2.12	Imperfection Of IQ Mixer . . . . .	9
<b>3</b>	<b>Data</b>	<b>10</b>
<b>4</b>	<b>Methodology</b>	<b>10</b>
4.1	Simulated Data . . . . .	10
4.1.1	Ideal Mixer . . . . .	10
4.1.2	Imperfect mixer . . . . .	12
4.1.3	Curve Fitting The Data . . . . .	12
4.2	Deriving Imbalance Data . . . . .	13
4.3	Mixer Data . . . . .	13
4.3.1	Study Data . . . . .	13
4.3.2	Data Under Test . . . . .	14
4.3.3	Calibration . . . . .	15
4.4	Vector Network Analyser Data . . . . .	16
<b>5</b>	<b>Results</b>	<b>16</b>
5.1	Study Data . . . . .	16
5.2	VNA Data . . . . .	16
5.3	Mixer Data Under Test . . . . .	18
5.3.1	SGS-SMF Data . . . . .	18
5.3.2	SGS Cable Loop-back - Data to be Calibrated . . . . .	18
5.3.3	SMF-SGS . . . . .	20
5.3.4	SMF Cable Loop-back - Data to be Calibrated . . . . .	20
5.3.5	Cable loopback of SMA . . . . .	20
5.4	Simulated Data . . . . .	20
5.4.1	Ideal Mixer . . . . .	20
5.4.2	Imperfect Mixer and Calibration . . . . .	21
<b>6</b>	<b>Conclusion</b>	<b>22</b>
<b>7</b>	<b>Critique of project</b>	<b>23</b>
7.1	Proposed Project . . . . .	23
7.2	Actual Project . . . . .	23
7.3	Unaddressed Objectives . . . . .	23
7.4	Time Management . . . . .	24
<b>8</b>	<b>Summary</b>	<b>24</b>

<b>9 Bibliography</b>	<b>25</b>
<b>A Appendices</b>	<b>27</b>
A.1 -30dB parameter data . . . . .	27
A.2 SMA-SGS parameter data . . . . .	28
A.3 SMA-SGS parameter data . . . . .	29

# 1 Introduction

## 1.1 Aim

This research project was aimed to calibrate and analyze a single Kinetic Inductance Detectors (KID) readout circuit. This readout circuit was combined with laptop in order to undertake the analysis and displayed the results of the input data. On successful completion of this analyzer, the plan is that to used it as portable test bed for AIG (Astronomy Instrumentation Group) laboratory in the future. The working principle of a KID is described in detail as when light is shone on the superconducting resonator it breaks the cooper pairs [1]. Cooper pairs were electron pairs bound together by a small energy equivalent to the energy of a mm-wave. So, a single low energy photon can split a cooper pair and create two normal unbound electrons known as quasi-particles. In the process as photons were absorbed by the detector it breaks the cooper pairs and thus increases the kinetic inductance and therefore modifies the resonante frequency  $F_0$ . A superconducting micro-resonator was used which is a phase sensitive homodyne readout method. The resonator serving as the detector was the simplicity of KID's case. Equivalent electrical diagram (1.1) is given below [2].

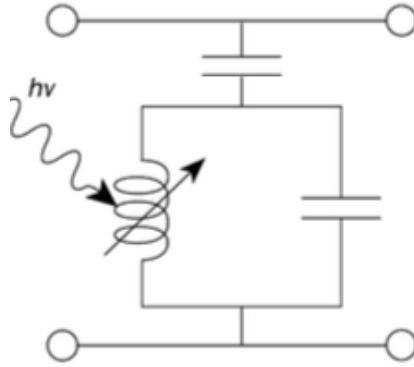


Figure 1.1: Equivalent circuit diagram of Kinetic Inductance detector [3]

As KID being LC resonator, they can be multiplied using frequency domain multiplexing method. Microwave transmission lines were used to couple multiple resonators and each resonator were designed to resonate at a unique frequency but varying the length of the capacitor legs. And the length of inductor was constant as the fractional change in inductance should be constant across the circuit for the given incident photon energy [4]. Diagram representation of the readout circuit is given below (1.2).

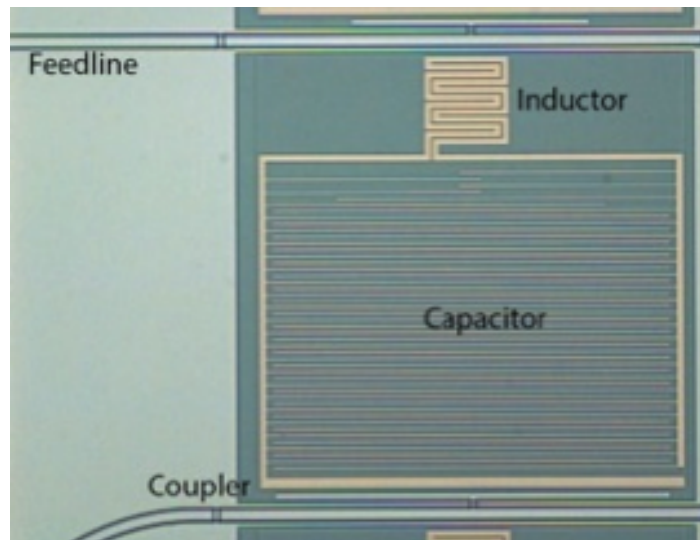


Figure 1.2: Kinetic Inductance detector [5]

KID was swept and measured through its scattering parameters S21 (2.6) using a homodyne system which measure the amplitude and a phase of a microwave signal propagated along a feed line past the KID. This was implemented by homodyne mixing.

Functionality of single mixer can be explained as when multiplying two signals it results in a trigonometric

function. Higher order frequency was filtered out and lower order frequency was used for the analysis. When two signals of same frequency were mixed the output of a single mixer is a DC voltage which is proportional to the phase difference between the two signals.

An IQ mixer is basically two mixers as shown in figure (1.3) where phase is delayed by 90 at the input of one mixer. Derived I and Q can be used to reconstruct the amplitude and phase of the wave which depend on the sample arm of the system.

## 1.2 Objective

To sweep out the KID, IQ mixer is used to trace out its resonant curve in S21 and then set a tone to the resonant frequency ( $F_0$ ) which is the minimum in S21. With a tone set to  $F_0$ , I and Q can be measures as a function of time and monitor how the amplitude and phase of the tone change as the KID resonance moves when its illuminated.

This methodology works if the mixer is perfect and for a perfect mixer the criteria are:

1. The phase angle between I and Q is 90 at all frequencies.
2. The relative gain or loss on both I and Q channels is the same at all frequencies.
3. There is no residual DC offset on I or Q.

Simulated codes were used to explain the how to model and demonstrate the impact of imperfection of the mixers. A simple length of transmission line was used as the simple for demonstrating the simulation.

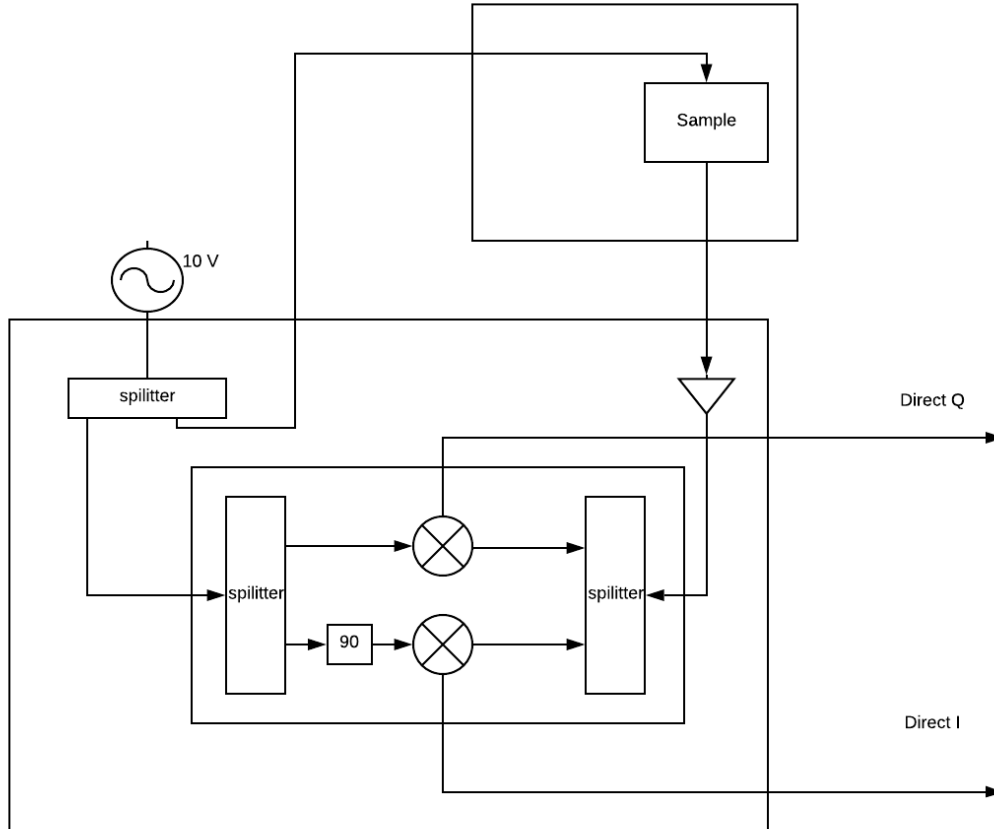


Figure 1.3: Block diagram of the readout circuit

This project analyze the sweep frequency of the KID which was the Device Under Test (DUT) to produce amplitude and phase response of the resonator. A tone was placed at the resonate frequency  $F_0$  and measures the changes in amplitude and phase of the signal as the resonator change shape due to change in inductance by photon absorption. This device can sweep in only one direction from port 1 to port 2 (S21). For accuracy

of the results, calibration was performed to the readings. The significance of this ideology was the portability of this readout circuit and replacement for Vector Network Analyzer (VNA) (2.4). And this project will be answering the research questions like,

1. Readout circuit replace the VNA in sweeping out the frequency.
2. Rate, performance speed and accuracy of readout circuit compared to VNA.
3. Used it as a detector for future astronomical instrumentation.

## 2 Précis of literature

### 2.1 Kinetic Inductance

The operational principle of KID is kinetic inductance. In electromagnetic force the charge carriers will oppose any charge using their inertia. The conductor's kinetic inductance is derived from Drude model [6].

$$\sigma = \frac{\sigma_0}{1 + \omega^2\tau^2} - i\omega\tau \frac{\sigma_0}{1 + \omega^2\tau^2} \quad (2.1)$$

$$\sigma_0 = \frac{ne^2\tau}{m} \quad (2.2)$$

where,

$n$  = charge carrier density

$e$  = electron charge

$\tau$  = collision time

$m$  = charge carrier mass

$\omega$  = frequency of wave in the conductor

From the equation above kinetic inductance is small unless the angular frequency of wave is large. The imaginary term of the conductivity becomes more significant as  $\tau \rightarrow \infty$  [4].

When photons with energy  $h\nu > 2\Delta$  hits the superconductor temporarily quasiparticles are made when the cooper pairs are broken by photon energy. When the quasiparticles are recombined to form cooper pairs the sheet impedance incident on the semiconductor increased due to the momentary reduction in charge carrier [7].

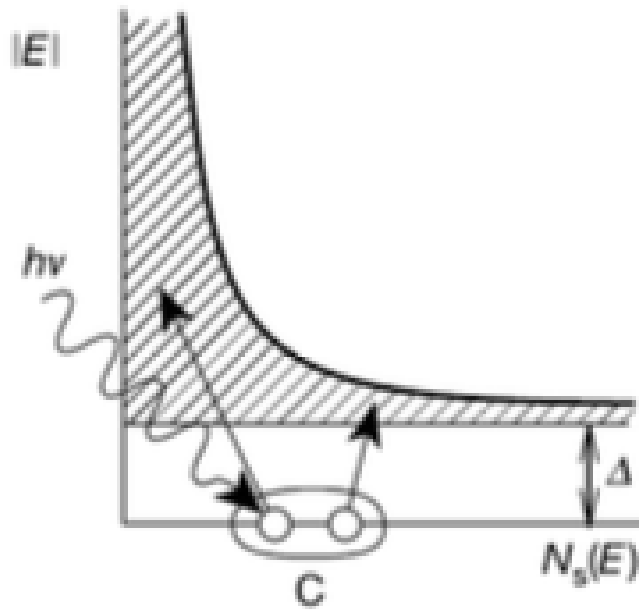


Figure 2.1: Diagrammatic representation of photons hitting the semiconductor and releasing quasiparticles [3]

## 2.2 Superconducting Microresonator

Microwave Kinetic Inductance Detector (MKID) also known as KID is an LC resonant circuit. They are capacitively or inductively coupled to a microwave transmission line (2.3). An equivalent circuit is mentioned above (1.1). When a photon of energy  $h\nu$  is incident on the superconducting inductor due to the kinetic inductance effect there will be an increase in the resonator inductance. Thus the frequency goes to  $\frac{1}{\sqrt{LC}}$  decreasing the resonant frequency and amplitude. This is measured using VNA (2.4) and is taken at the minimum amplitude of complex transmission of scattering parameter, S21 (2.6) [4]. This decrease is represented by the plot diagram below (2.2). The shift is also viewed in phase angle and is represented in the diagram below (2.3).

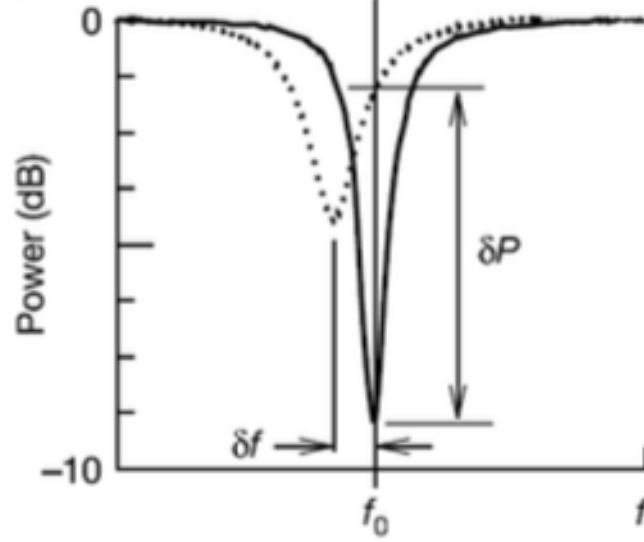


Figure 2.2: Resonate frequency change: Increase in inductance leads to decrease in resonant frequency and amplitude [3]

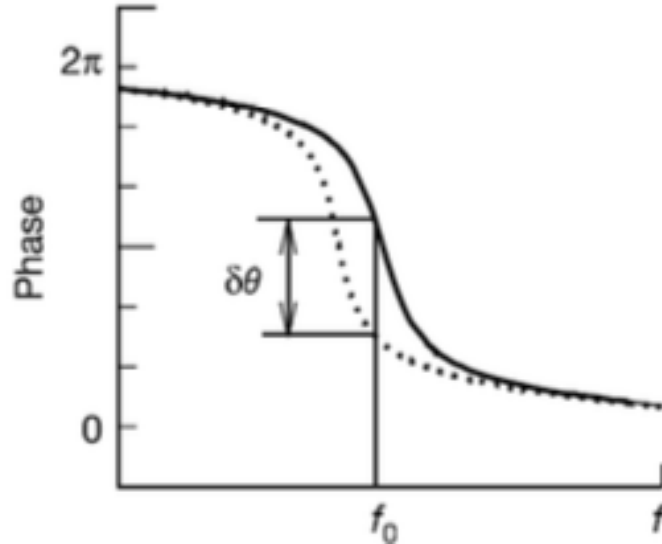


Figure 2.3: The phase shift due to the change in the signal [3]

## 2.3 Transmission lines

Transmission line has a major importance in the analysis of microwave circuits and devices. This distributed parameter network varies with voltage and current with respect to magnitude and phase over its length. They are always represented as two wired lines as shown in the figure below (2.4) as they have at least two conductors. A small line of length  $\delta z$  can be modeled as a lumped electronic circuit as shown in the diagram (2.5). [8] [9] R, L, G, and C are per-unit-length quantities defined as follows:

- $R$  = series resistance per unit length, for both conductors, in  $\Omega/\text{m}$ .
- $L$  = series inductance per unit length, for both conductors, in  $\text{H}/\text{m}$ .
- $G$  = shunt conductance per unit length, in  $\text{S}/\text{m}$ .
- $C$  = shunt capacitance per unit length, in  $\text{F}/\text{m}$ .

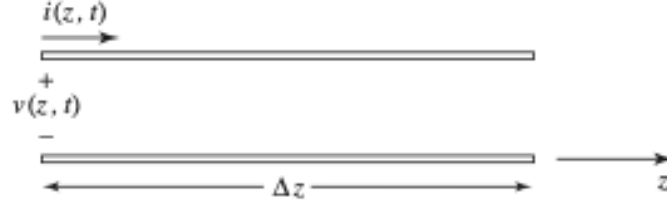


Figure 2.4: Transmission line representation [8]

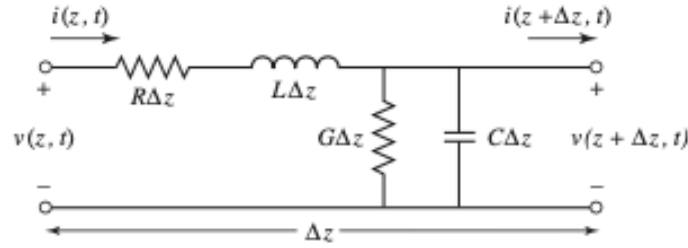


Figure 2.5: Equivalent electrical circuit for Transmission line [8]

## 2.4 Vector Network Analyzer

Vector Network Analyzers (VNA) are used to test component specifications and verify design simulations to make sure systems and their components work properly together. It has both source and receiver to it. Source is to send a known simulated signal to the DUT and a receiver port is to receive the signal from the DUT and analyze them. The measured results are processed later for deriving conclusions. A vector network analysis performs two types of measurements. One is transmission and the another is reflection. Transmission measurement passes the VNA simulated signal into the DUT and is measured by the receiver. The most common transmission measurements are S-parameter measurement. Using VNA the frequency sweep measurement at S-parameter is performed to the constructed readout circuit. Reflection measurement is the measurement of the signal which does not pass through the DUT and reflected back. Common reflection measurement s-parameters are  $S_{11}$  and  $S_{22}$  and transmission measurement s- parameters are  $S_{21}$  and  $S_{12}$  [10].

## 2.5 Scattering Matrix

The RF energy propagation through multi-port network is defined by scattering matrix. When the signal is incident on one port, some of the signals are reflected back and some excites at the other port being amplified or attenuated. The remaining energy left of the incident power are exited as heat and electromagnetic radiation. The S-matrix of N-port contains  $N^2$  coefficient called S-parameter (2.6). Each s-parameter represent a possible input-output path [11].

## 2.6 Principle Of S-parameter

The S-parameter is a complex number with real and imaginary part which can be used directly or in matrix form to show the reflection and transmission characterization of signal. This measurement is evaluated as amplitude and phase in the frequency domain. When a time varying signal is passed through a linear network the amplitude and phase value vary and they are helpful in frequency device characterization [12].



The four s-parameters of a two port network  $S_{11}, S_{12}, S_{21}, S_{22}$  are explained for their numerical convention as the first number following the S is the input port where the signal emerges and the second number is where the signal is applied. For example, in  $S_{21}$  port the port 1 is the input port and port 2 is the output port and for  $S_{11}$  port both the input and output port are the same [12].

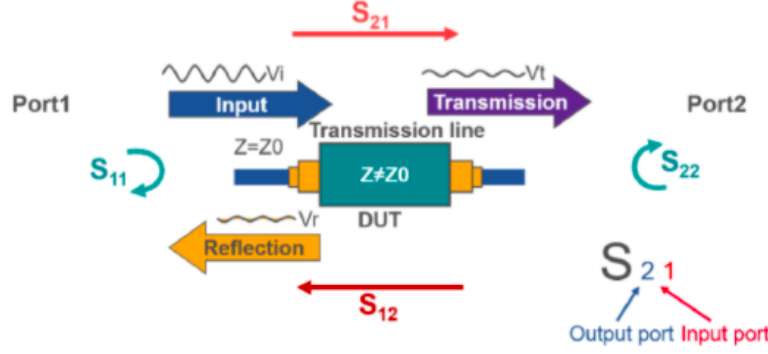


Figure 2.6: Working principle of s-parameter for a two-port network [12]

## 2.7 Calculating Scattering Parameter In Microwave Circuit

Microwave circuits are usually defined in terms of their scattering parameters. These define voltage waves entering and leaving a microwave circuit by their two ports. The change in impedance make part of the wave to reflect back. The DUT is placed between two ports of equal impedance (typically 50 Ohms). The scattering parameter defines the voltage waves entering one port and leaving another. For example, in a two-port system the DUT may be a piece of transmission line (2.3). If the line is lossless and matched to the port (50 Ohms) then  $S_{21} = 1$  and  $S_{11} = 0$ . If the line was matched to the port impedance but had some loss  $S_{21} < 1$  and  $S_{11}$  would be zero. If the line is not matched to the ports,  $S_{11} > 0$ . [13].

Scattering parameters are defined as the ratio of voltages on two ports. For  $S_{21}$  it is the ratio between port 2 and port 1. For the KID readout circuit these ports are used for the measurement of the amplitude and phase. These two ports will be separated by a cable if length L [14].

Voltage is applied across the terminals of port 1 of the form V (2.3) and measured at port 2. If the cable has a uniform impedance no power from the signal wave is reflected back to port 1 hence the voltage measured on port 2 is the same as port 1 and  $S_{21}$  (2.4). To calculate the phase difference in the ports, equation 2.5 is used where L is the length of the cable and  $\lambda$  is the wavelength of the signal passed in.

$$V = \sin(2\pi ft + \phi) \quad (2.3)$$

$$S_{21} = \frac{V_{out}}{V_{in}} = \frac{1}{1} = 1 \quad (2.4)$$

$$\phi = \frac{-2\pi L}{\lambda} \quad (2.5)$$

To calculate the scattering parameter of the KID, the KID is placed between the ports. As ports will be attached within the KID with minimum cable length leading to better result in calibrating  $S_{21}$ . Now theoretically assuming zero cable length by having  $L=0$ , the  $S_{21}$  parameter with respect to KID will be 2.7 where  $Q_r$  and  $Q_c$  are known as the resonator Q and coupling Q respectively and x is given by the equation 2.6 where  $F_0$  is the wave resonate frequency and F is the frequency of wave propagation along the line [8] [14].

$$x = \frac{F - F_0}{F_0} \quad (2.6)$$

$$S_{21} = 1 - \frac{Q_r}{Q_c} \frac{1}{1 + 2jQ_r x} \quad (2.7)$$

The I and Q components of  $S_{21}$  port can be obtained by simply getting the real and imaginary part of the the equation 2.7. This can be easily generated using python code [15]. Plotting it in the IQ plane will give a circle plot.

## 2.8 Introduction To Microwave Mixer

During the early radio days, crystal rectifiers were used as detectors. Later it was superseded by the thermionic value due to its constant necessity to adjust its point contact and poor efficiency. The very first microwave receiver used specially designed mixer. As noise preference is extremely important in microwave-based environment due to the very low signal encountered but in the microwave receiver as the frequency increased the output noise also increased. After multiple experiments it was found that crystal receivers used as mixers have high noise preferences than thermionic value at microwave frequency and many advancements were made with the mixer in later times for better performance. The improvements have resulted from better control over semiconductor purity, epitaxial material to achieve low series resistance and photo lithographic techniques to achieve small areas for Schottky diodes.

definition of mixer is the conversion of low power input signal combining it to a higher signal generated by Local Oscillator (LO) in a nonlinear device. As a result, the Intermediate Frequency (IF) is the sum and difference frequencies of the mixer. The difference frequency is of low power level and the sum is of higher power level. In microwave detection, solid state devices are used for direct refraction of input RF signal. Usually, the detectors sensitivity is much less than that of the receiver, but it is easily adjustable [16].

## 2.9 Mixers

A mixer is a non-linear or time variant element which is used to achieve frequency conversion. In ideal mixer when two signals are multiplied it produces output with respect to the sum and difference of the frequencies of the two input signals 2.8. For practical RF and microwave mixers the non-linearity is due to the operation of a diode or a transistor. To select the particular frequency range, filters are used and in modern mixers several filters are used to perform the up conversion and down conversion of the base band signal frequency and RF carrier frequency [8].

$$\cos(A)\cos(B) = \frac{1}{2}\cos(A+B) + \frac{1}{2}\cos(A-B) \quad (2.8)$$

For understanding the basic up conversion and down conversion operation of the mixer in frequency and time domain, trigonometrical identities are used. For up conversion, mixer multiplies a low-level input signal at one port with high level local oscillator (LO) at frequency  $\omega_{LO}$  as represented in figure (2.7). Multiplication is accomplished to create periodicity of the high lever local oscillator signal by on and off of the diode which created time varying conditions. The circuit is designed so that the time-varying conductance modulates the low-level input signal. This multiplication translates low level signal between the low intermediate frequency  $\omega_{IF}$  and at one port of the mixer and RF frequency  $\omega_{RF} = \omega_{LO} + \omega_{IF}$  [17].

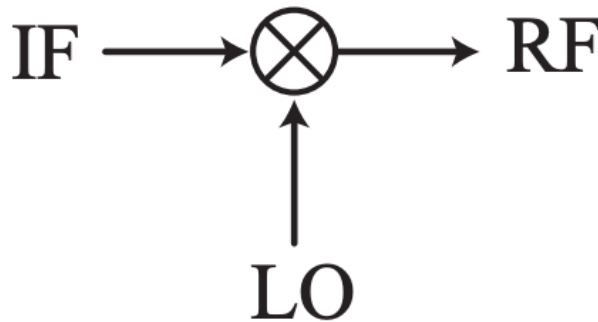


Figure 2.7: Mixer representation of up conversion [18]

### 2.9.1 Down Conversion Mixer

The down conversion is performed by mixing down the high frequency signals. When the desired output frequency is less than the input frequency it is called down conversion. The input port is driven by RF signal and the output port is driven by the intermediate IF signal as represented in the figure (2.8). The output is the difference of the RF frequency and LO frequency,  $\omega_{IF} = \omega_{LO} - \omega_{RF}$  [19].

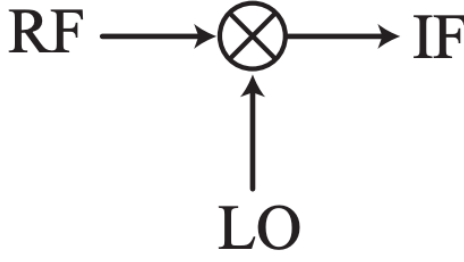


Figure 2.8: Mixer representation of down conversion [18]

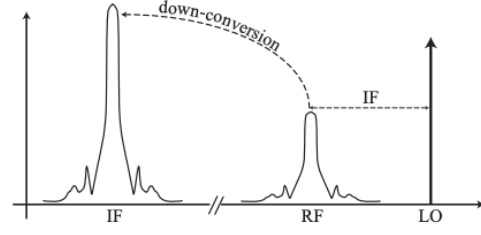


Figure 2.9: Graphical representation of down conversion [18]

Considering the equation of input signals as RF (2.9) and LO (2.10) and by recalling the trigonometric equation (2.11), the output  $\nu_{out}$  can be written as in equation below (2.13). The by grouping the terms we have the equation 2.14. The modulation is translated to two new frequencies  $LO + RF$  and  $LO - RF$ . Upper frequency or lower frequency is selected by using filter as shown in the figure (2.10). This process in simulated and filtered out using python code and explained in detail in the session (4.1.1) using the graphs 4.1 and 4.2

$$\nu_{RF} = A(t)\cos(\omega_0 t + \phi(t)) \quad (2.9)$$

$$\nu_{LO} = A_{LO}\cos(\omega_{LO}t) \quad (2.10)$$

$$\cos(A + B) = \cos A \cos B - \sin A \sin B \quad (2.11)$$

$$\nu_{out} = \nu_{RF}\nu_{LO} \quad (2.12)$$

$$\nu_{out} = \frac{A_t A_{LO}}{2} (\cos\phi(\cos(\omega_{LO} + \omega_0)t) + (\cos(\omega_{LO} - \omega_0))t - \sin\phi(\sin(\omega_{LO} + \omega_0)t + (\sin(\omega_{LO} - \omega_0)t))) \quad (2.13)$$

$$\nu_{out} = \frac{A_t A_{LO}}{2} (\cos((\omega_{LO} + \omega_0)t + \phi(t)) + \cos((\omega_{LO} - \omega_0))t + \phi(t))) \quad (2.14)$$

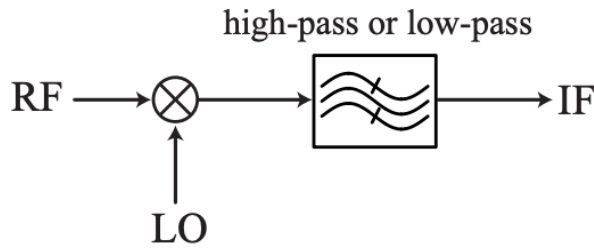


Figure 2.10: Mixer representation of with filter [18]

## 2.10 IQ Mixers

The IQ mixer consist of two mixers where the inputs RF and LO are connected to both the mixers one with in-phase power drive and another with quadrature hybrid. The output IF ports are considered as I for in-phase component and Q for 90° out-phase component and was modulated independently [20]. Diagram representation of IQ mixer is given below (2.11). Down conversation of the signal is performed by adding 50  $\Omega$  load to one of the port terminals. This down conversion method is used for homodyne detection.

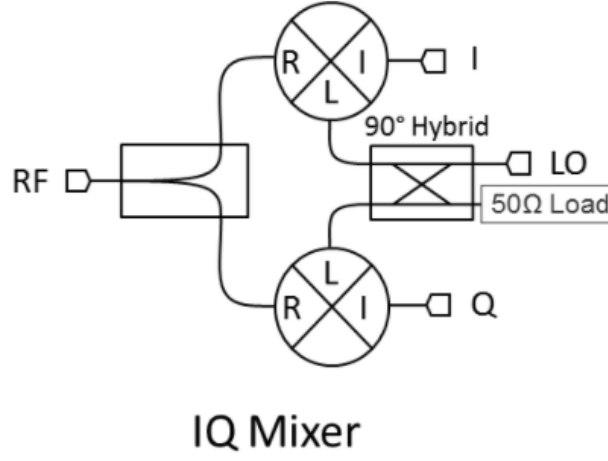


Figure 2.11: Diagram representation of IQ mixer [21]

### 2.11 IQ circle

IQ circles is a general plot between I and Q output values from the mixers as the frequency varies. The tone frequency can be set to one frequency and measure the IQ value and the tone of the frequency can be changed and the measured can be calculated for the new tone frequency. When there is no light incident on the KID the IQ mixer is static. . In the diagram (2.12) the line from the center of the circle to the circumference, the length is the amplitude and the angle is the phase of  $S_{21}$ . By finding the real and imaginary components of  $S_{21}$  parameter from the equation (2.7), amplitude (2.15) and phase (2.16) can be calculated. The IQ circle varies in position with respect to the cable length as it adds some phase. If a cable length adds  $45^\circ$  phase delay, the output measured will be in  $-45^\circ$ .

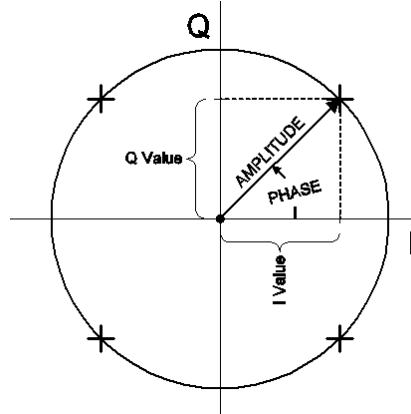


Figure 2.12: I vs Q plot [22]

$$\begin{aligned}
 S_{21}(\text{Amplitude}) &= \sqrt{(S_{21\text{real}})^2 + (S_{21\text{imaginary}})^2} \\
 &= \sqrt{(S_{21I})^2 + (S_{21R})^2}
 \end{aligned} \tag{2.15}$$

$$\begin{aligned}
 S_{21}(\text{phase}) &= \text{Arctan} \frac{S_{21\text{imaginary}}}{S_{21\text{real}}} \\
 &= \text{Arctan} \frac{S_{21Q}}{S_{21I}}
 \end{aligned} \tag{2.16}$$

### 2.12 Imperfection Of IQ Mixer

The imperfection of IQ circle is the DC-offset of I and Q ports. This is caused due to the convention loss imbalance between the two mixers of the IQ mixer. Other possible imperfections was Amplitude imbalance and phase imbalance. Amplitude imbalance is caused due to the unbalance in the quadrature coupler and different

conventional loss of the mixers the signal is not identical through the mixers. Phase imbalance is due to the unbalance in the hybrid coupler and the different electrical connection length [23].

With respect to the IQ circle, the imperfection can be identified as the shift for the origin of the IQ coordination system for DC-offset error. The calibration can be performed by adding external DC voltage to the I and Q ports or compensating the LO signal leakage. Amplitude imbalance or identified when the resulting IQ curve turn elliptical and for phase imbalance was identified by the change in phase angle. Slight modification in amplitude and phase of oscillating signal Q is performed for calibrating amplitude and phase imbalance.[24]. IQ plot representation of the error was shown in the diagram below (2.13).

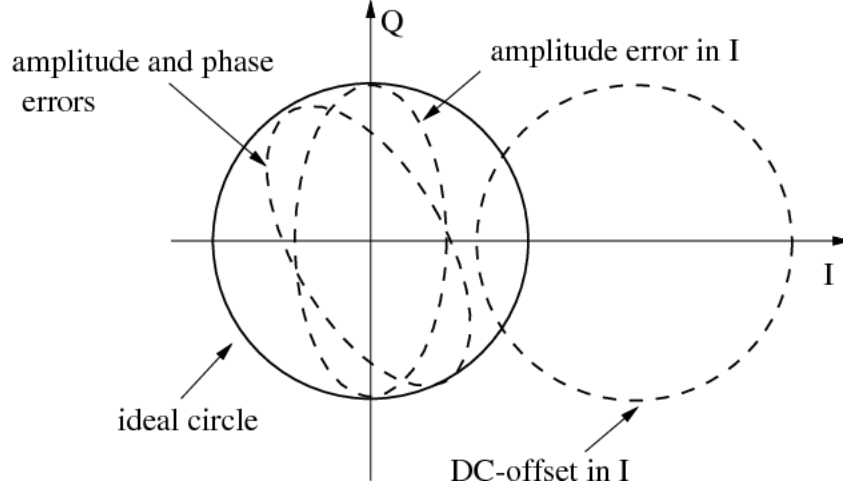


Figure 2.13: I vs Q plot with error imbalance [24]

### 3 Data

The data used in this project were taken in the AIG laboratory by a laboratory member. A already constructed mixer was used and analyzed for this project. Data obtained here was in ".fits" format and a special python package was used to unpack the files. Three different types of data were taken. They were mixer data, cable loop-back sweep data and VNA sweep data. The main data used here were the three synthesizer data used in mixer. These data were analyzed, calibrated and compared to each other for better understanding of the mixer.

## 4 Methodology

### 4.1 Simulated Data

#### 4.1.1 Ideal Mixer

Ideal mixers have a perfect quadrature signals which were 90° apart in phase with each other. They were also considered as lossless mixer and were simulated using python [15]. This helps us understand how a perfect I and Q signals looks. The simulation was performed by giving in the some known amplitude of LO signal and RF signal, known frequency of LO and RF signals, phase of LO and RF, sample frequency at which DAQ samples I and Q, number of points for simulation and time space with respect to simulation points. Now I and Q were calculated by giving in the formulae,

$$I = ((A_{LO} * A_{RF})/2) * (\sin(\omega_{LO} * t) + \Phi_{LO}) * (\sin((\omega_{RF} * t) + \Phi_{RF})) \quad (4.1)$$

$$Q = ((A_{LO} * A_{RF})/2) * (\sin(\omega_{LO} * t) + \Phi_{LO}) * (\sin((\omega_{RF} * t) + \Phi_{RF}) + (\pi/2.)) \quad (4.2)$$

where,

- $A_{LO}$  = Amplitude of LO
- $A_{RF}$  = Amplitude of RF

- $\omega_{LO}$  = Frequency of LO
- $\omega_{RF}$  = Frequency of RF
- $\Phi_{LO}$  = Phase of LO
- $\Phi_{RF}$  = Phase of RF
- $t$  = time points for simulation

By simulating I and Q using python and plotting both with respect to time space, the graph 4.1 is obtained. As it was the simulated signal it has both high frequency ( $\omega_{RF} + \omega_{LO}$ ) and the low frequency ( $\omega_{RF} - \omega_{LO}$ ). It was hard to inspect and analyze the required low frequency. Hence a low pass butter filter was used to filter out the required signal using python package SciPy signal. Low pass I and Q signal were represented in the figure 4.2 after the filtering process. Real life mixer has a filter at I and Q output which filters the high frequency signal and give the required low frequency. The quadrature signals were visible here and now this can be used for future analysis.

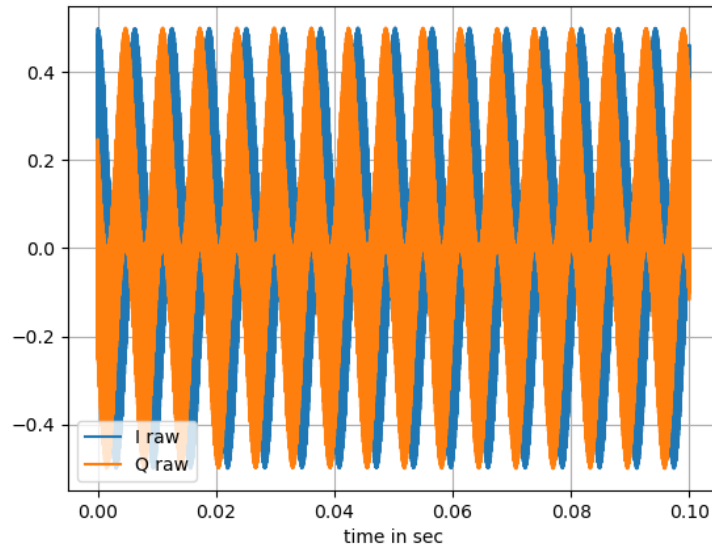


Figure 4.1: Simulated I and Q signals of a perfect mixer

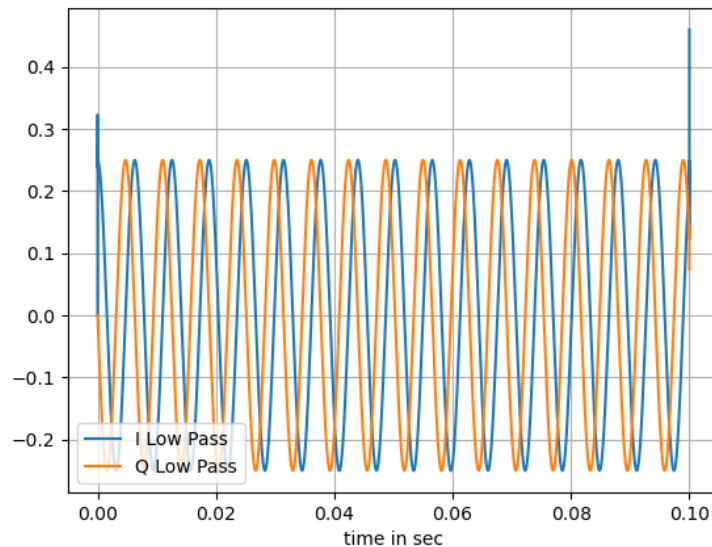


Figure 4.2: Simulated I and Q signals of a perfect mixer

### 4.1.2 Imperfect mixer

Same as an ideal mixer, an imperfect mixer can also be simulated using python just by adding some extra parameters like mixer loss, phase error and DC offset to the perfect I and Q. The formulae are given below.

$$I = ((M_{\text{loss}})(A_{\text{LO}} * A_{\text{RF}})/2) * (\sin(\omega_{\text{LO}} * t) + \Phi_{\text{LO}}) * (\sin((\omega_{\text{RF}} * t) + \Phi_{\text{RF}})) + DC_{\text{offset}} \quad (4.3)$$

$$Q = ((M_{\text{loss}})(A_{\text{LO}} * A_{\text{RF}})/2) * (\sin(\omega_{\text{LO}} * t) + \Phi_{\text{LO}}) * (\sin((\omega_{\text{RF}} * t) + \Phi_{\text{RF}} + (\pi/2.) + \theta_{\text{error}})) + DC_{\text{offset}} \quad (4.4)$$

where the parameters were same as 4.3 and 4.4 and the remaining were,

- $M_{\text{loss}}$  = Mixer loss
- $\theta_{\text{error}}$  = Phase error
- $DC_{\text{offset}}$  = DC offset

The graph 4.3 shown below the signal output of an imperfect mixer with DC off set of 2 voltage and Q being  $20^\circ$  out of phase and a mixer loss of 1. Other values can also be added into the simulation to study the imperfection of the mixer. In real time these imperfections were raised when a transmission line (2.3) of length L was added to the readout circuit. The delay form the signal due to its propagation through the transmission line will cause the imbalance in amplitude, phase and DC-offset. They were calculated and calibrated using scattering parameter  $S_{21}$  (2.7).

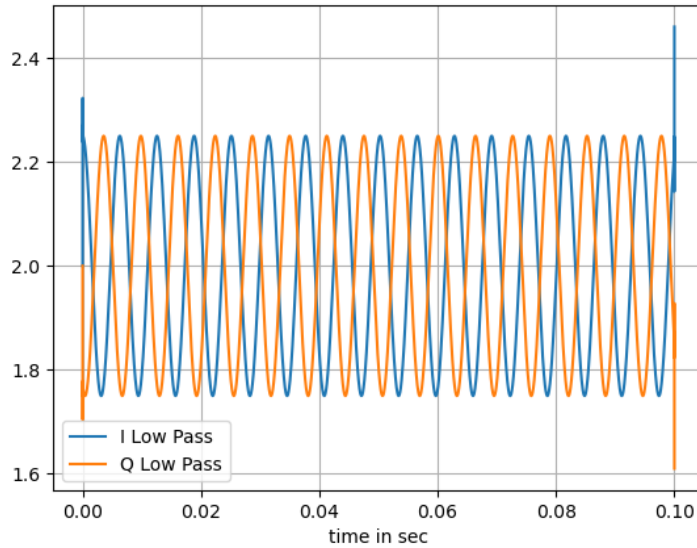


Figure 4.3: Simulated I and Q signals of a Imperfect mixer

### 4.1.3 Curve Fitting The Data

To the simulated imperfect mixer data a known range of DC offset, amplitude and phase errors can add and these signals can be fitted to a sine wave using python's curve-fit function and the parameters like Amplitude, phase and DC offset were retrieved with respect to the given sine function. The equation used for curve-fit function is 4.5. These derived amplitude, phase and DC offset values were used for analyzing the error and for calibrating the mixer.

$$A * np.\sin(w * t + p) + c \quad (4.5)$$

- A = amplitude of the signal
- w = period
- p = phase shift
- c = DC offset

## 4.2 Deriving Imbalance Data

The imperfection of amplitude imbalance, phase imbalance and DC offset were measured and accounted by measuring I and Q for RF and LO ports of the mixer run at a different frequency. The output on I and Q will be a sine wave at a frequency that was the difference in frequency between the input signals on the LO and RF ports,  $\omega_Q = \omega_I = \omega_{RF} - \omega_{LO}$ . For a perfect mixer the amplitude of I and Q should be the same and they should be 90 degrees out of phase with zero DC offset. Imperfect mixer output signal was fit to the perfect sine wave I and Q to measure the amplitude, phase and DC offset and therefore measure the non-ideal characteristics of the mixer.

## 4.3 Mixer Data

### 4.3.1 Study Data

The first set of mixer data were the LO port of the mixer was kept at 0dBm equivalent to 1mW of power and tested two different input powers on the RF port -20dBm and -30dBm to test and analyze the similarities and variation. Mixer data were stored as '. fits' file and the python package Astro Pi was used to unpack and analyzes these data. Header of each file can be accessed to extract the raw I and Q data and this raw data was fitted to a sine curve ( 4.5) and extract amplitude, phase and DC offset of the mixer for different frequencies were taken out. A negative amplitude gives the same result as a phase shift. For example,  $2*\sin(+0) = -2*\sin(+\pi)$ . Residual was calculated to indicate any error in the fit as a bad fit will lead to bad calibration values. This was indicated by high residual values.

The amplitude of I and Q data taken out from the fitted sine curve for each and every frequency individually for I data and Q data was plotted across the frequency individually. From the plot 4.4 it was clear that there was a small variation between I amplitude and Q amplitude. For a perfect mixer both the amplitudes should be same, and this proves that analyzed data was from an imperfect mixer. The next plot amplitude imbalance 4.5 which was calculated dividing I amplitude over Q amplitude. Here for this -20dB mixer data the difference was of the factor  $10^{-3}$ .

The phase shift value obtained for the curve-fit of I and Q signals were in radiant format. They were converted to degree format and their difference was plotted across frequency 4.6. This shows they were almost  $90^\circ$  out of phase from each other with some phase error to it. The graph 4.7 shows the phase error value plotted across the frequency in radiant.

The DC offset value of both I data and Q data were plotted 4.8 and by the graph it shows that there was a very slight vertical shift for both the signals. Residual was plotted 4.9 to verify how good was the curve-fit function works to the data points for both I and Q. As the residual number were very small it is a good fit.

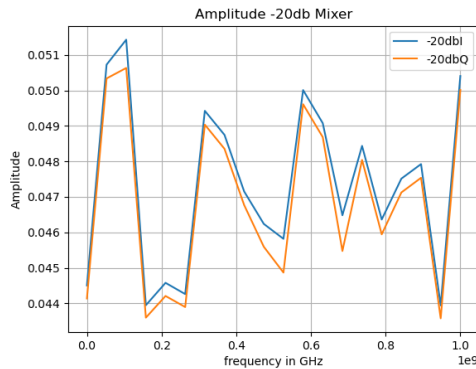


Figure 4.4: Amplitude Of I and Q data from fitted data

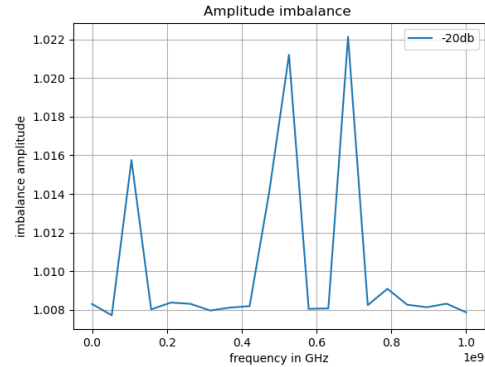


Figure 4.5: Amplitude imbalance of I and Q



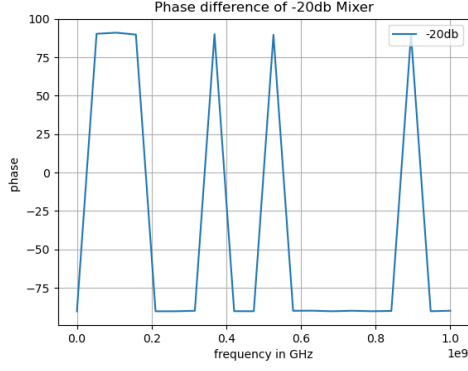


Figure 4.6: Phase difference Of I and Q data from fitted data

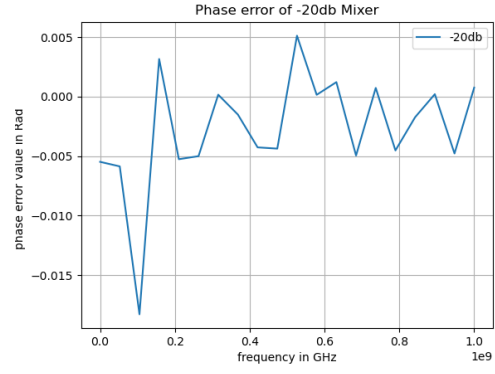


Figure 4.7: Phase error of I and Q

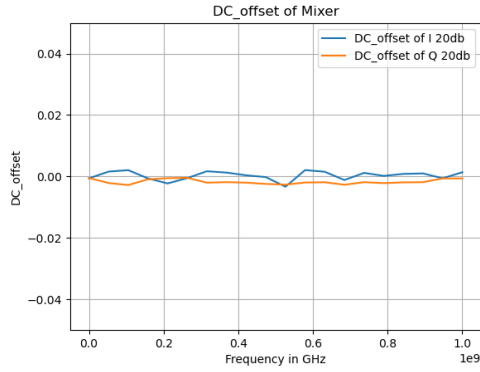


Figure 4.8: DC offset value Of I and Q data from fitted data

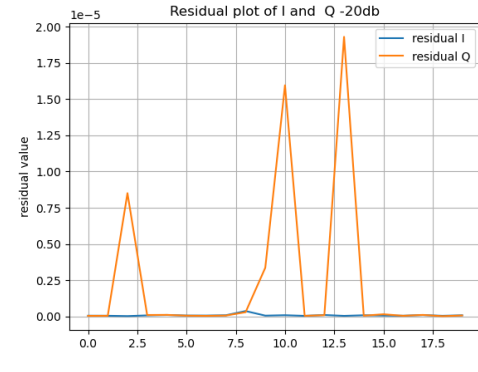


Figure 4.9: Residual from the fit of I and Q data to the sine function

### 4.3.2 Data Under Test

The two different ports of mixer were analyzed with three different synthesizers were used in mixer with two combinations of each for six measurements. One port was used as LO port and other port was used as RF port. The Synthesizers used were SGS, SMA, SMF. The mixer setup was shown in the diagram below (4.10.). Each synthesizer was used as synth 1 and synth 2 with six combinations as SGS-SMA, SGS-SMF, SMF-SMA, SMF-SGS, SMA- SGS, SMA-SMF and I and Q data were taken out for and were analyzed. These I and Q signals were fitted to a sine curve and their respective amplitude; phase shift and DC offset data were taken out for the individual frequencies. The graph derived from these data were analyzed to understand the working and performance of the mixer. The data to be calibrated and analyzed was the cable loop-back data of these three synthesizers.

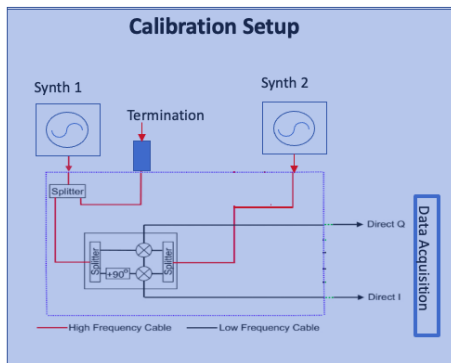


Figure 4.10: Mixer set up with synthesizers

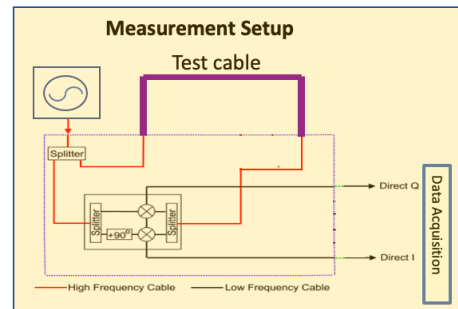


Figure 4.11: Measurement setup used test cable

### 4.3.3 Calibration

The I and Q data taken out from the callback sweeps were consisted to the raw I and raw Q and were calibrated with the amplitude, phase and DC offset obtained from the synthesizer mixer data. The calibration process for these data was of three steps. First the amplitude was corrected by using the amplitude imbalance data 4.6 calculated from the fitted data. The raw I was divided by the amplitude imbalance data if I was higher in amplitude than Q data 4.7. If I data was lesser in amplitude than Q data, then the amplitude imbalance data should be multiplied to the raw I data 4.8. The same method was used if Q was corrected from I.

$$A_{imb} = A_I/A_Q \quad (4.6)$$

$$I_{raw} = \frac{I_{raw}}{A_{imb}} \quad (4.7)$$

$$Q_{calibrated} = Q_{raw} * A_{imb} \quad (4.8)$$

where,

- $A_{imb}$  = Amplitude imbalance
- $A_I$  = Amplitude obtained from fitted data
- $A_Q$  = Amplitude obtained from fitted data
- $I_{raw}$  = I data from the loop callback sweep
- $Q_{raw}$  = Q data from loop callback sweep

The second step was to correct the DC offset by subtracting the fitted DC offset value of I and Q data from the raw I 4.9 and Q 4.10 data.

$$I_{raw} = I_{raw} - IDC_{off} \quad (4.9)$$

$$Q_{calibrated} = Q_{raw} - QDC_{off} \quad (4.10)$$

where,

- $IDC_{off}$  = DC offset of I from the fitted data
- $QDC_{off}$  = DC offset of Q from the fitted data

The third set is to correct the phase imbalance. This was done by calibrating either Q or I with respect to the other phase. The equation for the calibration was given below 4.15. First the magnitude 4.11 and angle 4.12 of I raw and Q raw was measured. Then to find the change in Q signal as  $\Delta Q$  4.13 angle, magnitude and phase error measured from the fitted data were used. The calibrated Q ( $Q_{cal}$ ) was obtained from the equation 4.14 and then finally for scaling up the small loss in the process equation 4.15 was used.

$$Magnitude = \sqrt{I_{raw}^2 + Q_{raw}^2} \quad (4.11)$$

$$A_{measured} = \text{Arctan} \frac{Q_{raw}}{I_{raw}} \quad (4.12)$$

$$\Delta Q = Magnitude * \sin(\theta_{error}) * \cos(A_{measured}) \quad (4.13)$$

$$\begin{aligned} Q_{cal} &= Q_{raw} + \Delta Q \quad \text{if I was positive} \\ Q_{cal} &= Q_{raw} - \Delta Q \quad \text{if I was negative} \end{aligned} \quad (4.14)$$

$$Q_{cal} = Q_{cal} * \frac{1}{\cos(\theta_{error})} \quad (4.15)$$

## 4.4 Vector Network Analyser Data

Vector network analyzer (VNA) data was considered to be the proper and the measurement of test cable will be compared to the VNA data. The VNA data were different compared to the mixer data. the real part of VNA was considered as the I data and the imaginary part of VNA was considered as the Q data. The S21 plot 4.12 was the magnitude of the real and imaginary values of the VNA and the phase plot 4.13 was the arctan of imaginary data over real data. I vs Q plot 4.14 should that the data has no amplitude imbalance, phase imbalance or DC offset.

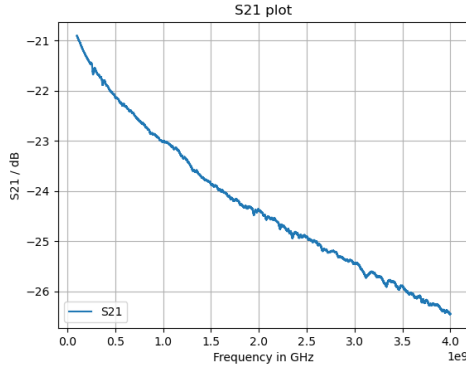


Figure 4.12: Magnitude plot of VNA data

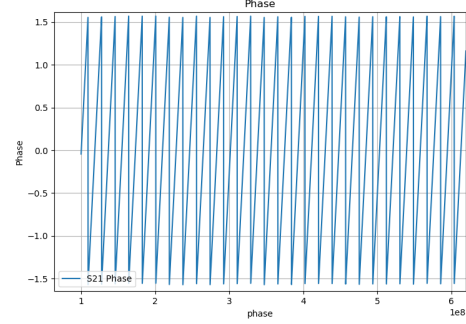


Figure 4.13: Phase plot of VNA data

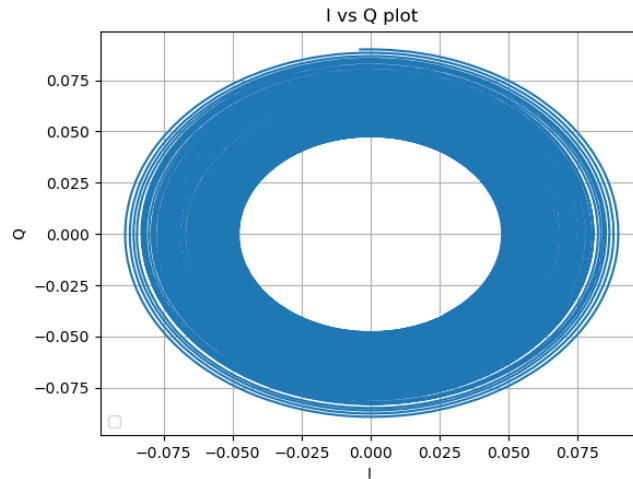


Figure 4.14: I vs Q plot of -20db VNA data

## 5 Results

### 5.1 Study Data

First tested data -20dB and -30db were plotted across each other to understand the difference. As the power given in was of the difference 10 db the result obtained should be around same difference. Plotting the magnitude of -20db and -30db (5.1), it shows that the magnitude plots were of the difference -10db with respect to the powers given in.

The amplitude plot 5.2 shows the the variation in power in dB. And as the phase 5.3 and DC offset 5.4 would not differ with respect to the power given it they look similar with minimal loss for both -20db and -30db.

### 5.2 VNA Data

VNA analysis and measurements were considered to be the right measurement and our mixer calibrated data should like VNA data. Three plots magnitude, phase and I vs Q were plotted. The magnitude plot 5.5 decreases

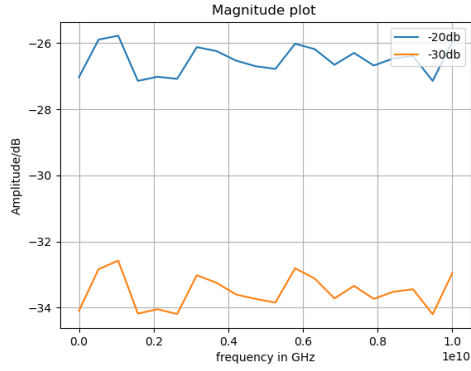


Figure 5.1: Magnitude plot of -20db and -30db data

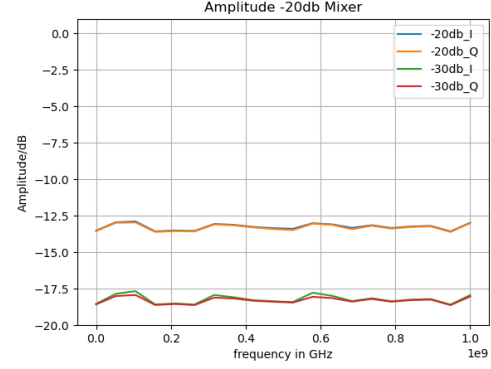


Figure 5.2: Amplitude plot of both I and Q for -20db and -30db

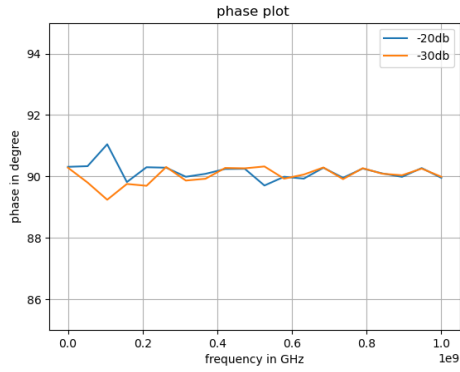


Figure 5.3: phase plot of both -20db and -30db

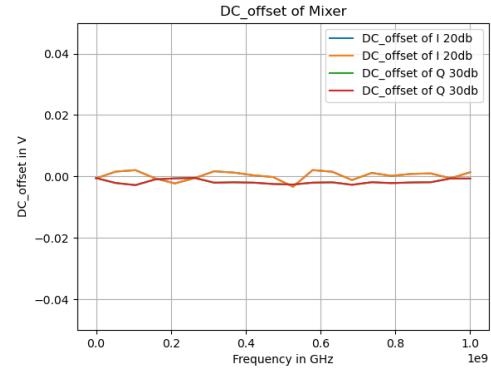


Figure 5.4: DC offset plot of both -20db and -30db

from -0.4dB to -1.1dB across the frequency. The curve has little bumps and dips as there will be other factor affecting the measurement in minor level. Here the overall shape of  $S_{21}$  curve was observed and not the absolute value, as it depends on the overall mixer loss. And the phase [5.6](#) varies from  $+90^\circ$  and  $-90^\circ$  proving that they were  $90^\circ$  apart from each other. The I vs Q plot [5.7](#) were smooth and was a proper circle. This proves that there was no amplitude imbalance, phase shift or DC offset to this data.

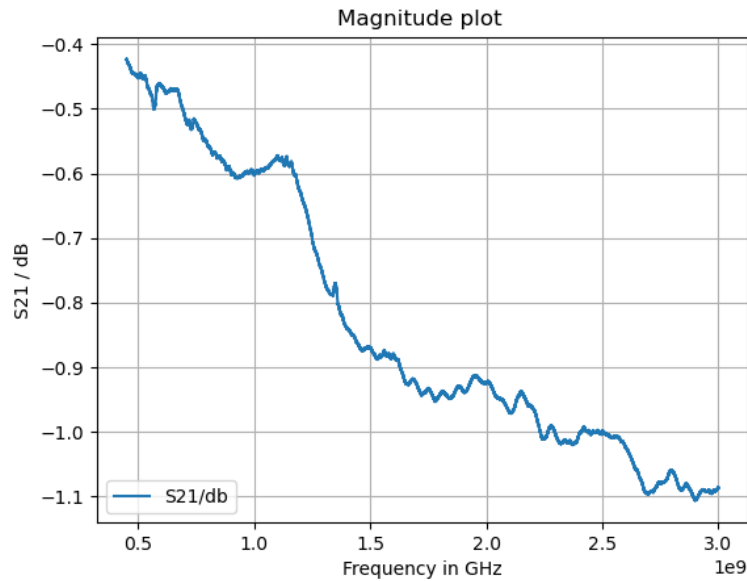


Figure 5.5: S21 magnitude plot

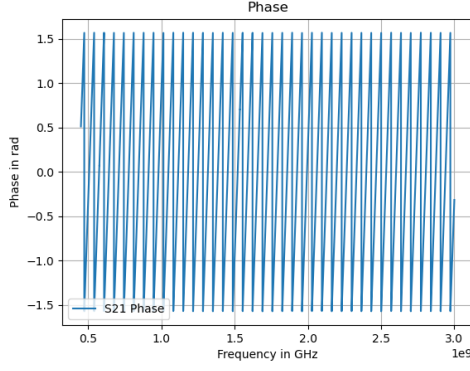


Figure 5.6: Phase plot

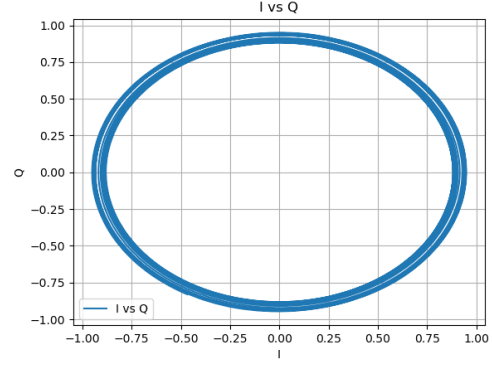


Figure 5.7: I vs Q plot

## 5.3 Mixer Data Under Test

### 5.3.1 SGS-SMF Data

The mixer data that was analyzed using synthesizers SGS-SMF in the ports. After fitting the data and extracting the values from the fit, amplitude imbalance, phase difference and magnitude of the amplitudes were calculated and plotted as the function of frequency. These plots can give rough idea in the credibility of the data.

Amplitude imbalance 5.8 which was calculated I over Q shows almost 1 from the plot with a minor variation of  $10^{-3}$ . This shows that the amplitude of I and Q is almost same just with a difference of factor  $10^{-3}$ . And the magnitude plot 5.9 shows that the power of output signal is of range -3db to -5db. This range was maintained thorough the frequency range. Thus, the mixer has very minimal loss.

The difference between I and Q signals should always be  $90^\circ$  as there were with respect to the construction of the mixer. The difference was always  $90^\circ$  other than three frequencies as shown in the plot 5.10. This difference was due to the the bad fit at those three frequencies. Dc offset of Q was much flat ie, close to zero then DC off set of I 5.11. Overall, the DC offset value of both I and Q was neat and flat with 0.005 volt shift in I and 0.001 volt shift in Q. The phase error in those three frequencies seems to be only in phase difference and other plots in that frequencies were good. Overall, this mixer data has a good fit and values were considered good for calibration.

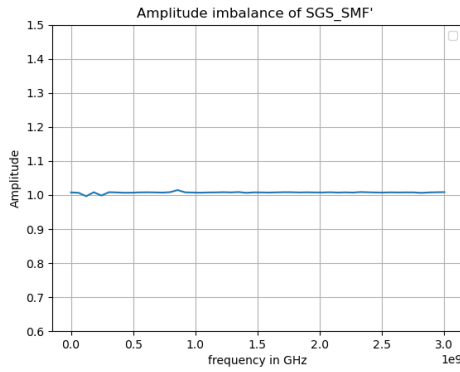


Figure 5.8: Amplitude imbalance of SGS-SMF mixer data

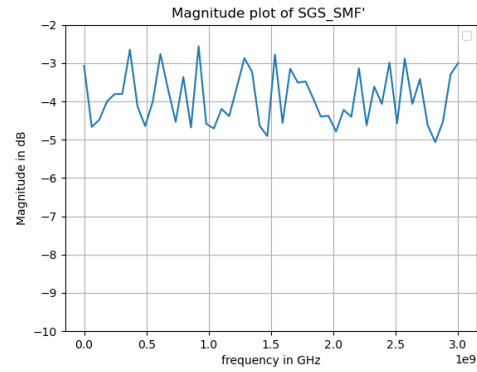


Figure 5.9: Magnitude of SGS-SMF mixer data

### 5.3.2 SGS Cable Loop-back - Data to be Calibrated

The I and Q signals from cable loop-back data should be calibrated using the Amplitude imbalance, phase error and DC offset calculated using two synthesizers SGS-SMF. First amplitude 4.7 was calibrated then DC offset 4.9 and 4.10 was calibrated. Then the phase imbalance was calibrated using 4.15. After performing calibration, then magnitude 5.12 of calibrated I and Q was calculated and plotted for analysis. The plotted magnitude graph was not similar to the VNA magnitude graph. Next the phase 5.13 of calibrated I and Q was measured and plotted. Phase calibration looks similar to the VNA data. Finally plotting the I vs Q circle 5.14 it shows

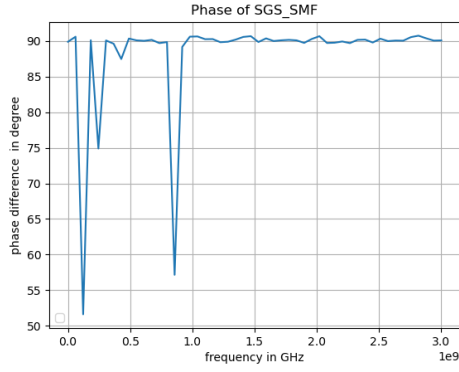


Figure 5.10: Phase of SGS-SMF mixer data

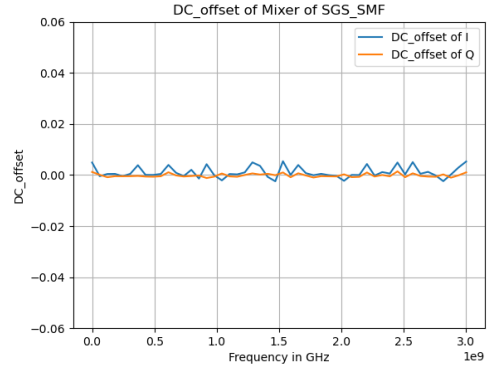


Figure 5.11: DC offset value of SGS-SMF mixer data

that there was not DC offset as the circle was centered and the phase shift was hard to figure out in this figure. The phase plot show that the phase was calibrated. And with the elliptical circles in the I vs Q circle it was clear that the data has a huge amplitude error.

The amplitude imbalance of this mixer data was almost 1 thought the frequency and was also represented by a graph 5.8. A small error like this should not make there many ripples in the magnitude. These ripples could be by some other factor other than the mixer. For further clarification other data were also analyzed, calibrated and plotted below.

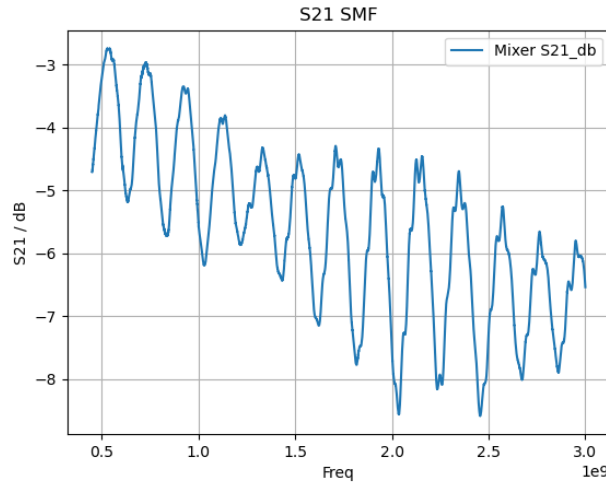


Figure 5.12: Magnitude of SMF mixer data

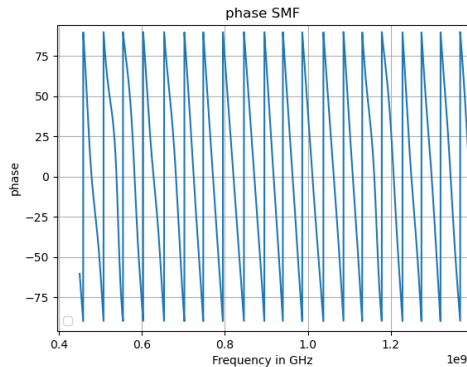


Figure 5.13: Phase of SMF mixer data

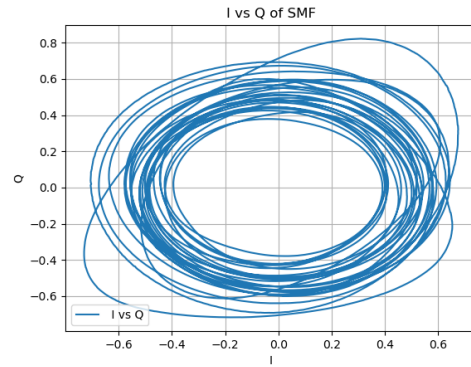


Figure 5.14: I vas Q plot of SMF data

### 5.3.3 SMF-SGS

Here the amplitude imbalance [5.15](#) plot and magnitude plot [5.16](#) looks good. The phase error plot [5.17](#) looks little unstable whereas the DC offset [5.18](#) value was neat.

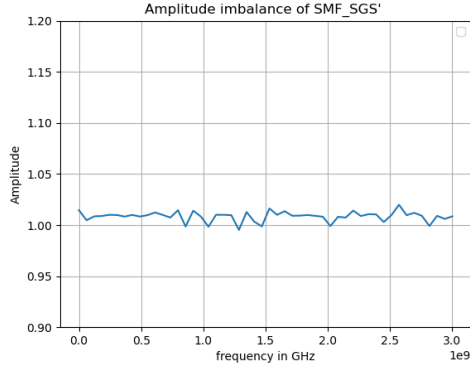


Figure 5.15: Amplitude imbalance of SMF-SGS- mixer data

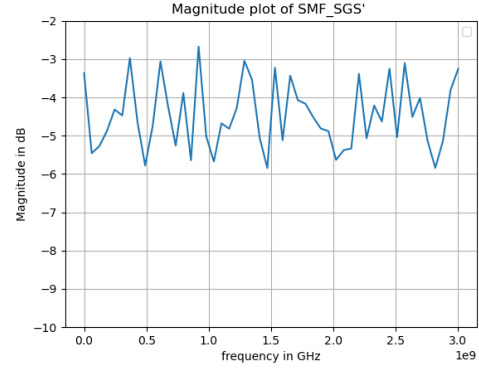


Figure 5.16: Magnitude of SMF-SGS mixer data

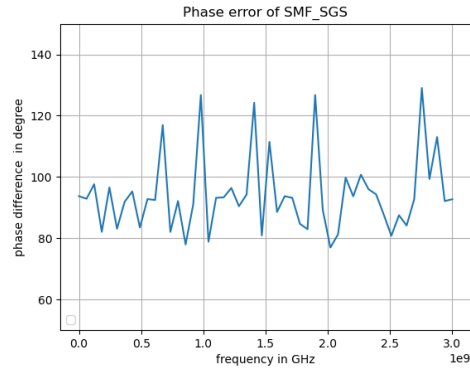


Figure 5.17: Phase of SMF-SGS mixer data

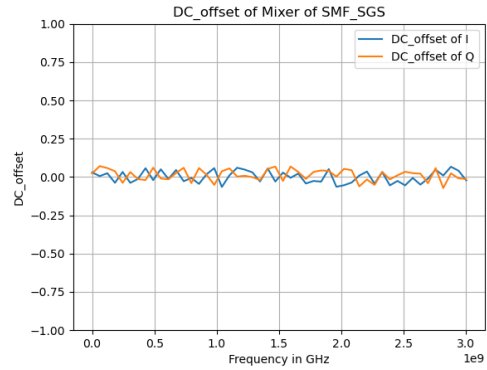


Figure 5.18: DC offset value of SMF-SGS mixer data

### 5.3.4 SMF Cable Loop-back - Data to be Calibrated

Here again the phase [5.20](#) and DC off from the I vs Q circles shows [5.21](#) that the data were calibrated properly but again the magnitude plot [5.19](#) have lot many ripples and in I vs Q plot they have lot many elliptical shape. Now it was more likely that there was an external noise to the mixer which was making these ripples.

### 5.3.5 Cable loopback of SMA

Even the cable loop-back data for both SMA-SGS [5.22](#) mixer and SMA-SMF [5.23](#) mixer give a similar result with lot of ripples. This gives a high possibility of error outside the mixer. For the calibration method, the same calibration method can be used to a simulated data and the phase and magnitude plots can be analyzed.

## 5.4 Simulated Data

### 5.4.1 Ideal Mixer

There were two possibilities for the magnitude with high noise. One the calibration method should have some problem to it. Two the mixer data used for testing should have some external error to it which makes the ripple for all the data. This can be verified by simulating an ideal mixer and calculating the S21 magnitude plot [5.24](#), phase plot [5.25](#) and the I vs Q plot [5.26](#) and assuming these calculation as perfect plots as similar to VNA. The magnitude S21 graph was smooth gradually decreasing with frequency and the phase varies uniformly throughout the frequency with  $+90^\circ$  and  $-90^\circ$  variation between I and Q signals. The I vs Q plot

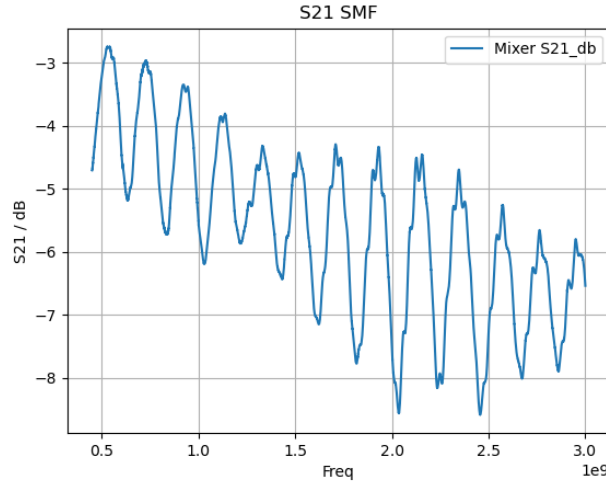


Figure 5.19: Magnitude of SMF mixer data

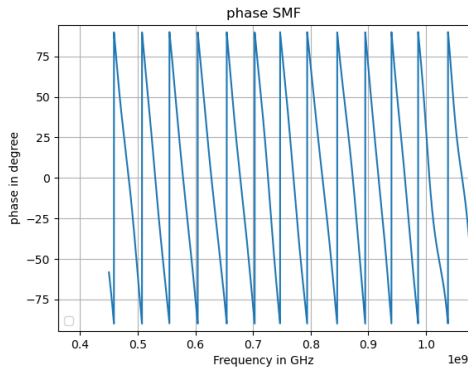


Figure 5.20: Phase of SMF mixer data

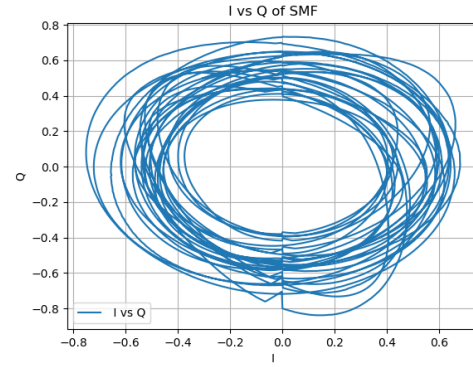


Figure 5.21: I vs Q plot of SMF data

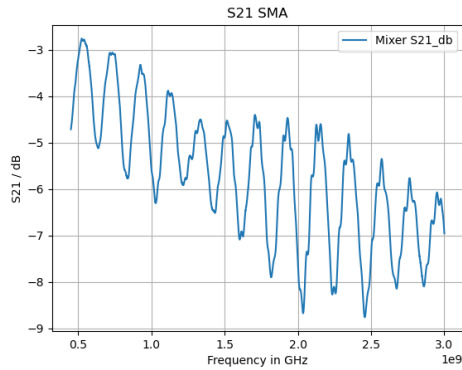


Figure 5.22: Calibrated magnitude for SMA-SGS mixer

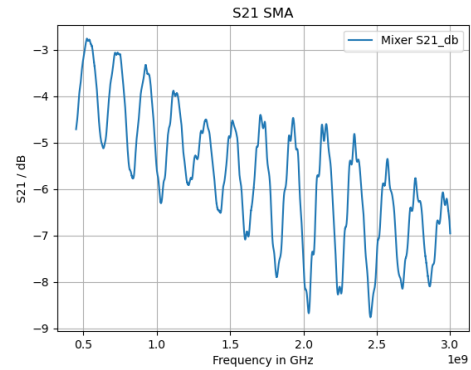


Figure 5.23: Calibrated magnitude for SMA-SMF mixer

was spherical implementing there was no amplitude imbalance or phase imbalance or DC offset to this ideal mixer simulated data.

#### 5.4.2 Imperfect Mixer and Calibration

An imperfect mixer was simulated by adding in know amplitude imbalance, phase shift and DC offset. These signals were fitted to a sine function and corrected amplitude, phase and DC offset were taken out. Now these values were used to an imperfect mixer and calibrated for amplitude imbalance. phase imbalance and DC offset. Then the calibrated value was calculated for S21 magnitude [5.27](#) and phase [5.28](#).

From the graphs it was clear that both ideal mixer calculations and calibrated imperfect mixer data look same.



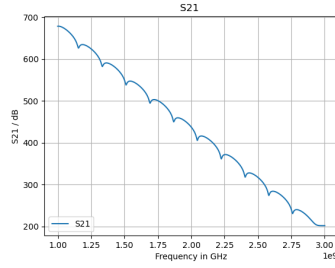


Figure 5.24: S21 magnitude polt of an ideal mixer

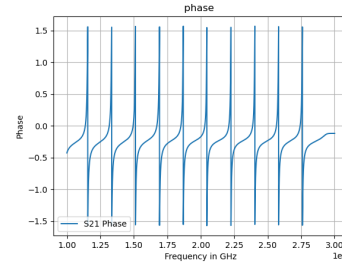


Figure 5.25: Phase plot of an ideal mixer.

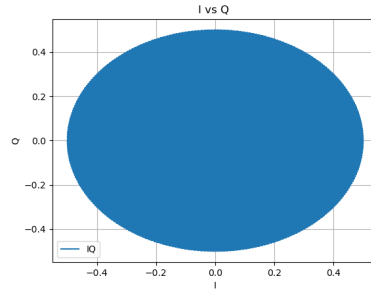


Figure 5.26: I vs Q plot of an ideal mixer

This proves that the calibration works. The raw mixer data should have some external factor affecting it other the mixer itself.

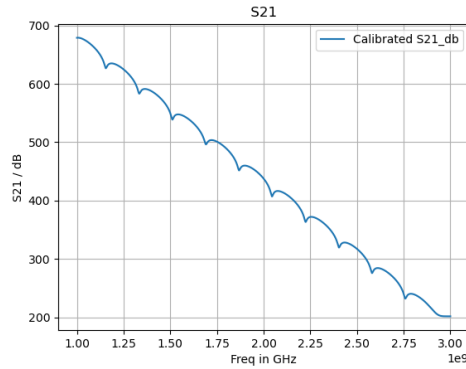


Figure 5.27: S21 magnitude polt of an calibrated mixer

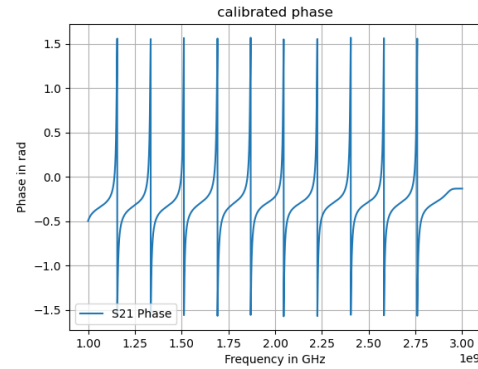


Figure 5.28: Phase plot of an ideal mixer.

## 6 Conclusion

The calibration model constructed using python for the project works perfectly for simulated ideal and non-ideal mixer. All six-cable loop-back data shows the same ripple through the S21 magnitude graph concluding that there was an external factor that causes the ripple.

The first proof used for this conclusion was that the amplitude imbalance calculated from the fit parameter has a value to it, meaning there was a very difference between I signal and Q signal. For a mixer to be perfect both the amplitude value of I and Q should be same. After performing amplitude imbalance calibration to the cable loop-back data there was not much difference in the output. whereas the phase imbalance calibration and DC offset calibration works perfectly. The only problem here was the magnitude value. As any difference amplitude will not affect the phase and DC offset of the mixer. The second proof was by checking the calibration method to a simulated non-ideal mixer and comparing it with an ideal mixer output. The non-ideal mixer was calibrated and the output looks similar to ideal mixer. This proves that calibration method works per-

fectly. This leaves to the conclusion that the problem was in the cable loop-back data and external to the mixer.

Even though the calibration works it cannot be concluded that this analysis mythology can be used as a replacement for Vector Network Analyzer. Even with a different cable loop-back data it cannot be concluded as a replacement. More mixer data have to be used and tested under different conditions. The calibration method should show good accuracy rate for all the conditions. Only then this model can be considered as a replacement. Even with a different cable loop-back data it cannot be concluded as a replacement. More mixer data have to be used and tested under different conditions. The calibration method should show good accuracy rate for all the conditions. Only then this model can be considered as a replacement.

Possible future work for the project was to analyze more mixer data and also to calculate mixer loss and the cable length. Accuracy of the model should improve, and this entire python script can be covered into a LabView [25] project makes this model user friendly. On successful completion of the above can be tested as a detector for astronomical instruments.

## 7 Critique of project

### 7.1 Proposed Project

The project was proposed to construct a single Kinetic Inductance Detector readout circuit from the scratch and calibrate it by analyzing the I and Q data generated by the readout circuit. The objective of the project was to measure and sweep the KID at different frequencies to produce amplitude and phase response of the resonator. And the objectives were to,

1. Analyzing IQ data.
2. Calibrate and characterize the mixer under required frequency
3. Developing a program for replacing VNA in the sweeping process of the frequency.
4. Portability of the KID readout circuit.

Later on, the proposal was modified a little due to COVID-19 restrictions. As the accessibility of lab was uncertain the entire project was modified as remote based project. A constructed mixer was used in the KID circuit and the reading was taken and given for the analysis.

### 7.2 Actual Project

Before working with the actual data for the project, a brief study about the analysis process was done with simulated data to understand the mixer behavior. Then second study data was with -20dB and -30dB data, which took longer than the expected time to analyze and conclude them. Then finally the mixer data generated with the different synthesizers were given for analysis which were the actual data have to be analyzed with the project. By the time a proper working python code was constructed and was used for the mixer data. The addressed objectives were,

1. A complete analysis of IQ data was performed
2. Calibration and characterization were partially performed.

The Gantt chart demonstrating the project timeline with the data given time and the analysis time mentioned.

### 7.3 Unaddressed Objectives

The objectives that were not achieved were,

1. The developed python program was not able to replace the sweeping process of VNA.
2. Portability of KID circuit is also a question as the previous objective was not achieved.



Figure 7.1: Gantt chart demonstrating the project timeline

These objectives were not able to address as the calibration of the mixer did not work perfectly. The error was first thought to be in the analysis process and later as the same error was in all the data set it was conducted that the error was outside the mixer and at that time of period new data sets were not able to be taken and analyzed. Thus, this led to being unable to compare or replace the developed program to the VNA for the sweep process and thus that caused being unable to port the KID readout circuit.

## 7.4 Time Management

With the Actual plan and a normal circumstance, the time allocated for this project would be better. With the pandemic and the lockdown, it was hard to keep in track of the project. Understanding the methodology itself was quite challenging and doing the project remotely was hard to meet the deadlines. There were also a lot of personal issues that made the project lag back in time. Shift of place, fall sick also were the major factors for the delay in the project. In particular more time was spent with the analysis of the sample data than originally planned. That made a short availability of time for the final calibration.

## 8 Summary

This project deals with analyzing, calculating and calibrating a mixer by using three different synthesizers. The synthesizers were used in two combinations each of six in total where they were given to mixers LO and RF ports. Then a cable was connected to the one of the ports removing one synthesizer and a cable loop-back sweep was measured which was to be calibrated for identifying mixer performance.

Simulated ideal and imperfect mixer data helped in better understanding of the working process of the IQ mixer. A known power of -20dB and -30dB was given to the mixer and analysis was performed with that data. Parameters were taken out from the fitted data and were plotted to examine and understand them. The magnitude graph shows the difference in dB concluding that difference in power given into the mixer. Residuals were calculated to check the fit of the mixer data to the sine function. Both -20dB and -30dB had a perfect fit with the residual value of order  $10^{-8}$  to  $10^{-9}$ . Mixer data using synthesizers were calculated for obtaining the parameters from the fit and plotted across frequency for analyzing them. Then the error from the parameters was used to calibrate the cable loop-back data to check the performance of calibration and mixer. The synthesizer data has some external error to it, the calibration method did not work. This was checked by implementing the calibration method for an imperfect mixer simulated value with the known error. As the calibration method works it is concluded that the given data has external error other than the mixer error to it.

## 9 Bibliography

### References

- [1] Baselmans, J. Kinetic inductance detectors. *Journal of Low Temperature Physics* **167**, 292–304 (2012).
- [2] Zmuidzinas, J. Superconducting microresonators: Physics and applications. *Annual Review of Condensed Matter Physics* **3**, 169–214 (2012).
- [3] Day, P. K., LeDuc, H. G., Mazin, B. A., Vayonakis, A. & Zmuidzinas, J. A broadband superconducting detector suitable for use in large arrays. *Nature* **425**, 817–821 (2003).
- [4] Szypryt, P. *Development of microwave kinetic inductance detectors for applications in optical to near-IR astronomy* (University of California, Santa Barbara, 2017).
- [5] UCSB Physics - Redirection Page URL <https://web.physics.ucsb.edu/~bmazin/mkids.html>.
- [6] Bloch, F. Quantum mechanics of electrons in crystal lattices. *Z. Phys* **52**, 555–600 (1928).
- [7] Mazin, B. Microwave kinetic inductance detectors ph. d. thesis (2004).
- [8] Pozar, D. M. *Microwave engineering; 3rd ed.* (Wiley, Hoboken, NJ, 2005). URL <https://cds.cern.ch/record/882338>.
- [9] Paul, C. R. *Analysis of multiconductor transmission lines* (John Wiley & Sons, 2007).
- [10] Hernández, R., Loayssa, A. & Benito, D. Optical vector network analysis based on single-sideband modulation. *Optical Engineering* **43**, 2418–2422 (2004).
- [11] URL <https://www.microwaves101.com/encyclopedias/s-parameters>. Date accessed : 2021-05-25.
- [12] Schweber, B. What are the functions and principles of s-parameters (part 1)? (2019). URL <https://www.analogictips.com/what-are-the-functions-and-principles-of-s-parameters-part-1/>. Date accessed : 2021-05-26.
- [13] Martens, J. *et al.* Flux flow microelectronics. *IEEE transactions on applied superconductivity* **3**, 2295–2302 (1993).
- [14] Understanding kinetic inductance detector microwave readout. *article* .
- [15] Van Rossum, G. & Drake, F. L. *Python 3 Reference Manual* (CreateSpace, Scotts Valley, CA, 2009).
- [16] Anand, Y. & Moroney, W. J. Microwave mixer and detector diodes. *Proceedings of the IEEE* **59**, 1182–1190 (1971).
- [17] Williams, D. F., Ndagijimana, F., Remley, K. A., Dunsmore, J. A. & Hubert, S. Scattering-parameter models and representations for microwave mixers. *IEEE transactions on microwave theory and techniques* **53**, 314–321 (2005).
- [18] Niknejad, A. M. Introduction to mixers URL [http://rfic.eecs.berkeley.edu/~niknejad/ee142\\_fa05lects/pdf/lect15.pdf](http://rfic.eecs.berkeley.edu/~niknejad/ee142_fa05lects/pdf/lect15.pdf).
- [19] Nickolas, C. The basics of mixers (2011). URL <https://www.digikey.in/en/articles/the-basics-of-mixers>.
- [20] URL <https://www.markimicrowave.com/iq-mixers/iq-mixers-products.aspx>. Date accessed : 2021-05-26.
- [21] Jorgesen, D. & Jorgesen, D. How to think about iq mixers (2019). URL <https://www.markimicrowave.com/blog/how-to-think-about-iq-mixers/>.
- [22] Wolke, b. What’s your iq – about quadrature signals... (2015). URL <https://www.tek.com/blog/quadrature-iq-signals-explained>. Date accessed : 2021-05-26.
- [23] Rubio, A. R. (0AD).

- [24] Sabah, S. & Lorenz, R. Design and calibration of iq-mixers. In *EPAC*, vol. 98, 1589 (Citeseer, 1998).
- [25] Bitter, R., Mohiuddin, T. & Nawrocki, M. *LabVIEW: Advanced programming techniques* (Crc Press, 2006).

# A Appendices

## A.1 -30dB parameter data

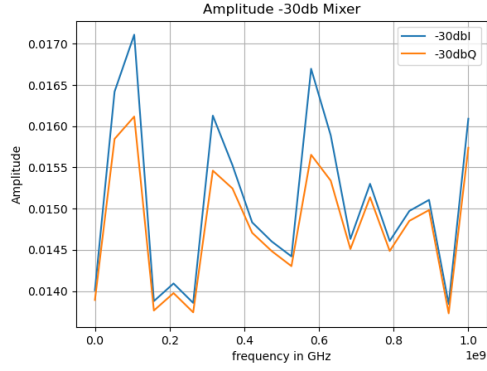


Figure A.1: Amplitude of -30dB

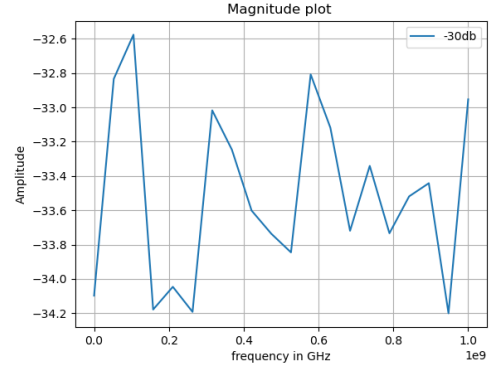


Figure A.2: magnitude of -30dB

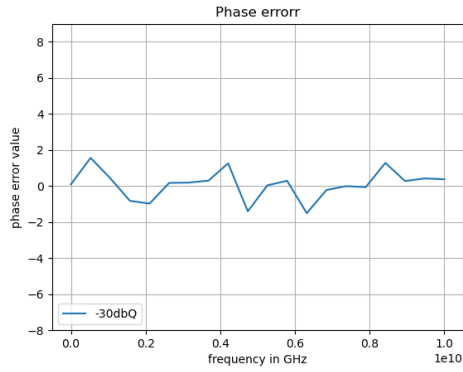


Figure A.3: phase error of -30dB

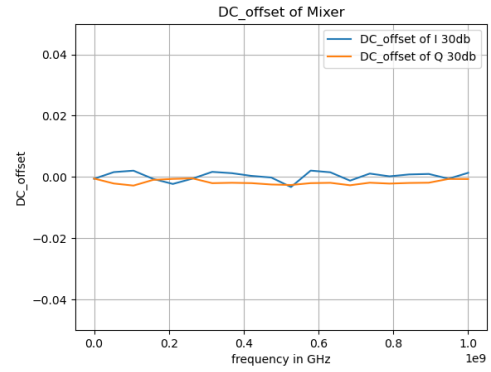


Figure A.4: DC offset of -30dB

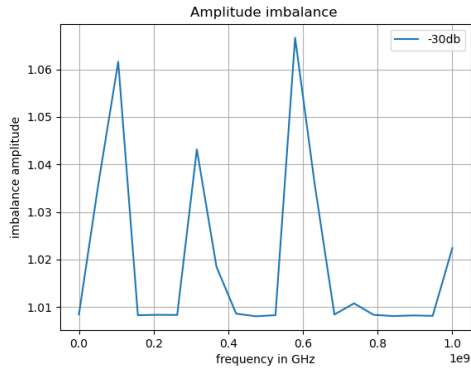


Figure A.5: Amplitude imbalance of -30dB

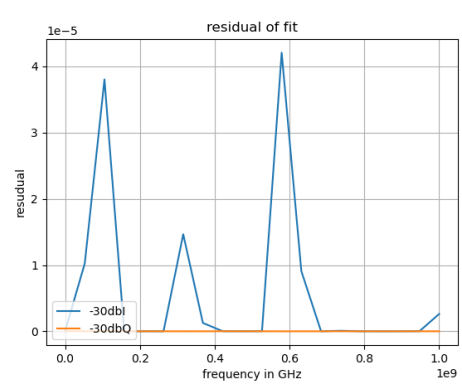


Figure A.6: residual plot

## A.2 SMA-SGS parameter data

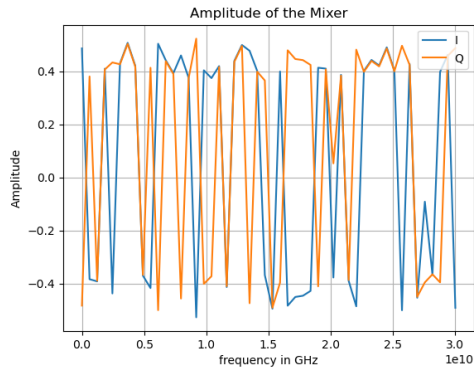


Figure A.7: Amplitude of the mixer

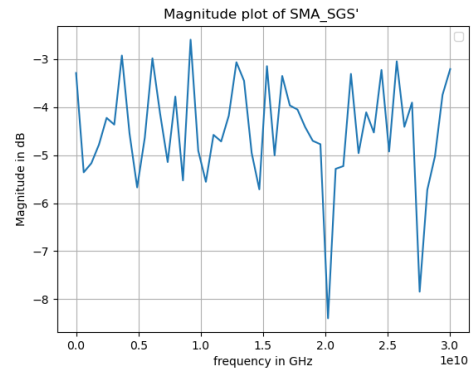


Figure A.8: magnitude of mixer

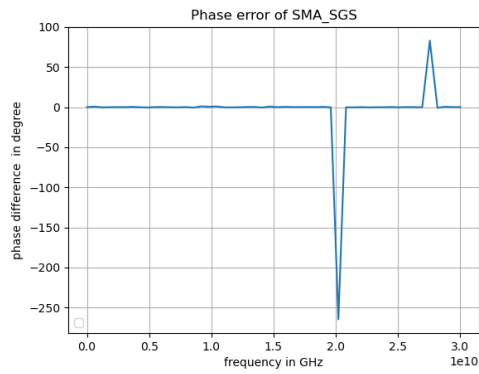


Figure A.9: phase error of mixer

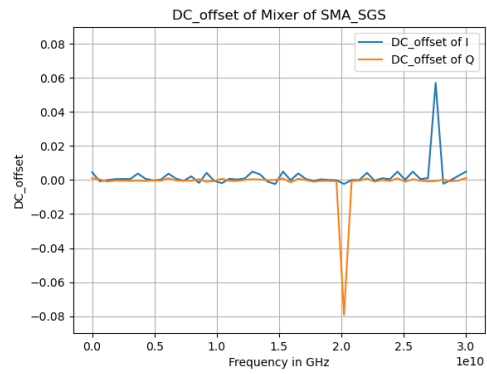


Figure A.10: DC offset of mixer

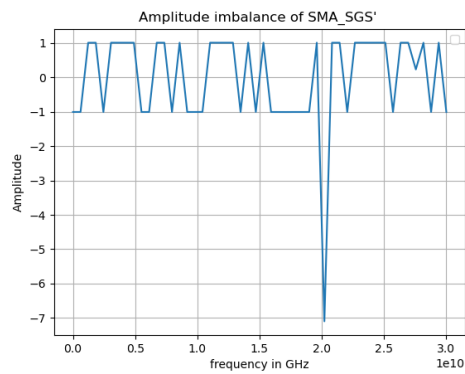


Figure A.11: Amplitude imbalance of mixer

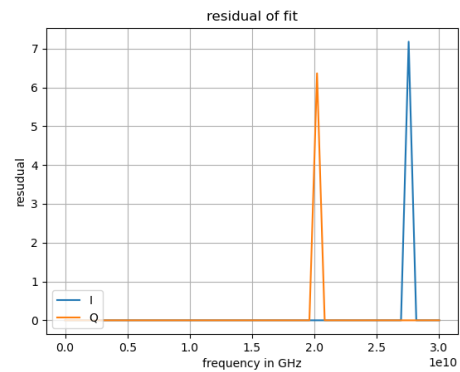


Figure A.12: residual plot

### A.3 SMA-SGS parameter data

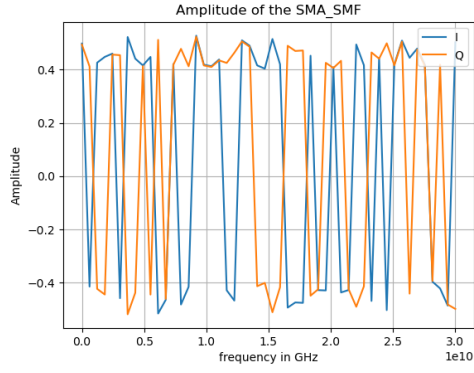


Figure A.13: Amplitude of the mixer

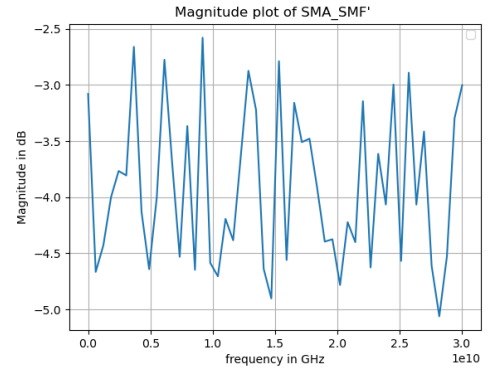


Figure A.14: magnitude of mixer

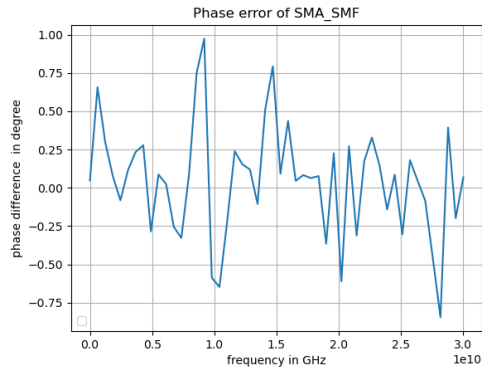


Figure A.15: phase error of mixer

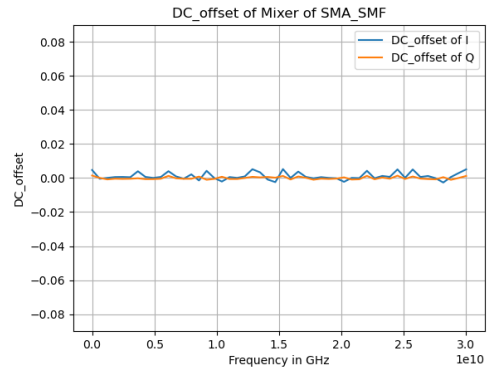


Figure A.16: DC offset of mixer

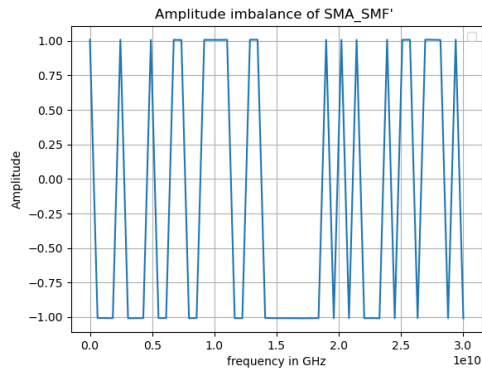


Figure A.17: Amplitude imbalance of mixer

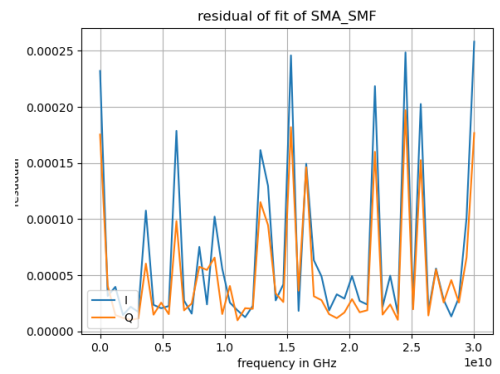


Figure A.18: residual plot